

Electronic Supplementary Informations

1. General method

All chemicals and solvents were purified according to the standard procedure.^[S1] DCC was purchased from Sinopharm group Ltd., *p*-toluidine was purchased from J&K Scientific Ltd. Compounds **1a**, **1b**, **2a** and **2b** were synthesized according to our previous report.^[S2]

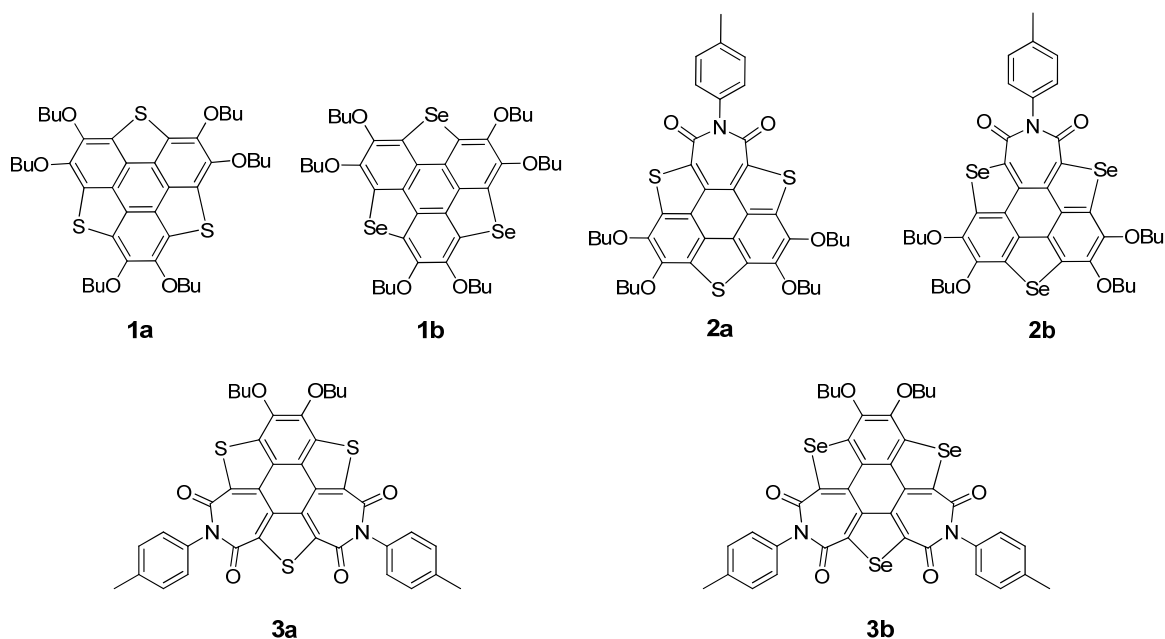
Melting points were determined on WRS-2 melting point apparatus. ¹H and ¹³C NMR spectra were recorded on a Bruker Advance III 400MHz (100 MHz for ¹³C) spectrometer using CDCl₃ as solvent. The chemical shifts of ¹H and ¹³C NMR were recorded using TMS as internal standard. High resolution mass spectral analysis (HRMS) was carried out on Bruker APEX II type mass spectrometer. UV-Vis spectra were measured on UV-2006 UV-Specterophotometer. Fluorescence excitation and emission spectra were recorded with an RF-5301(pc)s Spectrofluorophotometer, fluorescence lifetime and steady state were measured on FLS920 Spectrofluorophotometer. All of the measurements were conducted in the CH₂Cl₂ solution (10⁻⁵ mol L⁻¹) at 20 °C.

All calculations were carried out with the *Gaussian 16* suite of programs.^[S3] For DFT calculations, we used the hybrid gradient corrected exchange functional of Lee, Yang, and Parr. A standardized 6-311G basis set was used together with polarization (d) and (p) functions.^[S4]

References

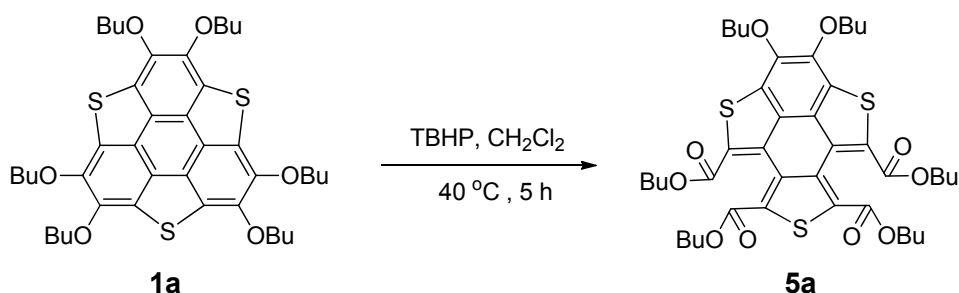
- [S1] *Purification of Laboratory Chemicals*, 5th ed., Wilfres L.F. Armarege, Christina L.L.Chai.
- [S2] a) X. Li, Y. Zhu, J. Shao, B. Wang, S. Zhang, Y. Shao, X. Jin, X. Yao, R. Fang, X. Shao, *Angew. Chem. Int. Ed.* **2014**, 53, 535–538; b) X. Li, Y. Zhu, J. Shao, L. Chen, S. Zhao, B. Wang, S. Zhang, Y. Shao, H.-L. Zhang, X. Shao, *Angew. Chem. Int. Ed.* **2015**, 54, 267–271.
- [S3] *Gaussian 16, Revision A.03*, M. J. Frisch, G. W. Trucks, H. B. Schlegel, G. E. Scuseria, M. A. Robb, J. R. Cheeseman, G. Scalmani, V. Barone, G. A. Petersson, H. Nakatsuji, X. Li, M. Caricato, A. V. Marenich, J. Bloino, B. G. Janesko, R. Gomperts, B. Mennucci, H. P. Hratchian, J. V. Ortiz, A. F. Izmaylov, J. L. Sonnenberg, D. Williams-Young, F. Ding, F. Lipparini, F. Egidi, J. Goings, B. Peng, A. Petrone, T. Henderson, D. Ranasinghe, V. G. Zakrzewski, J. Gao, N. Rega, G. Zheng, W. Liang, M. Hada, M. Ehara, K. Toyota, R. Fukuda, J. Hasegawa, M. Ishida, T. Nakajima, Y. Honda, O. Kitao, H. Nakai, T. Vreven, K. Throssell, J. A. Montgomery, Jr., J. E. Peralta, F. Ogliaro, M. J. Bearpark, J. J. Heyd, E. N. Brothers, K. N. Kudin, V. N. Staroverov, T. A. Keith, R. Kobayashi, J. Normand, K. Raghavachari, A. P. Rendell, J. C. Burant, S. S. Iyengar, J. Tomasi, M. Cossi, J. M. Millam, M. Klene, C. Adamo, R. Cammi, J. W. Ochterski, R. L. Martin, K. Morokuma, O. Farkas, J. B. Foresman, and D. J. Fox, Gaussian, Inc., Wallingford CT, 2016.
- [S4] a) A. D. Becke, *J. Chem. Phys.* **1993**, 98, 5648; b) C. Lee, W. Yang, R. G. Parr, *Phys. Rev. B* **1988**, 37, 785; c) V. A. Rassolov, M. A. Ratner, J. A. Pople, P. C. Redfern, L. A. Curtiss, *J. Comp. Chem.* **2001**, 22, 976.

2. Synthesis

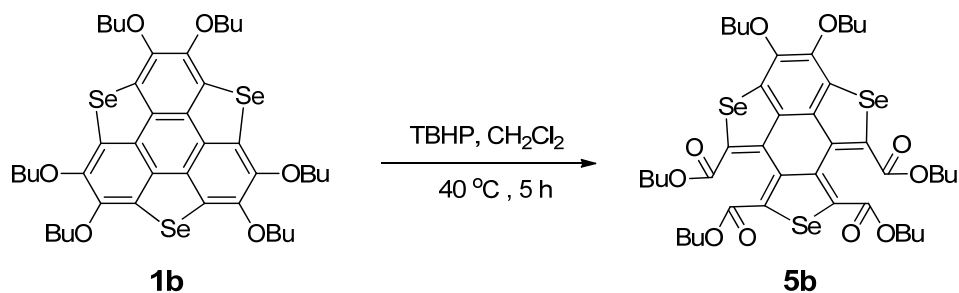


Scheme S1. The chemical structures of the compounds in this report.

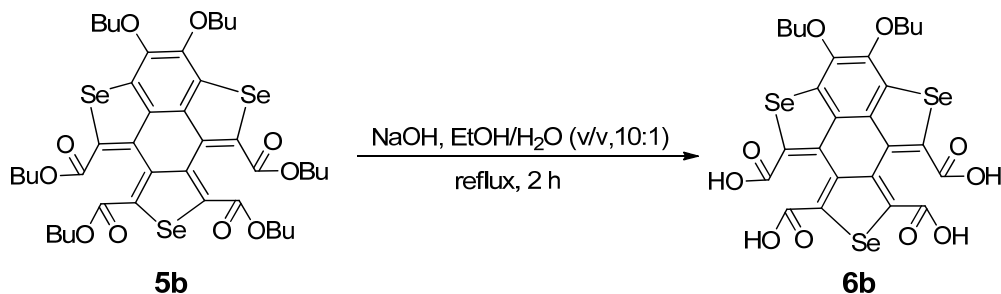
Experimental details:



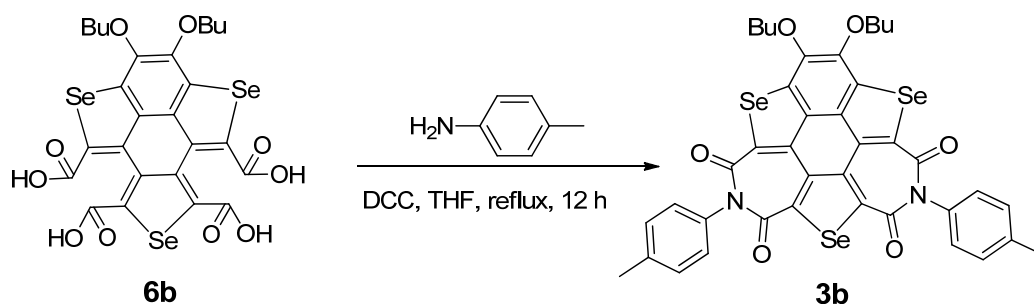
Compound **1a** (75 mg, 0.1 mmol) and TBHP (*tert*-butyl hydroperoxide, 4 drops) were dissolved in CH_2Cl_2 (10 mL). The resulting mixture was stirred at 40 °C for 5 h. After cooled down to RT, the reaction was quenched by adding distilled water and extracted with CH_2Cl_2 (3×15 mL). The organic layers were combined and dried over anhydrous Na_2SO_4 , then concentrated under reduced pressure. The crude product was further purified by column chromatography on silica-gel (eluent, CH_2Cl_2 : petro ether, 2 : 1, v/v) to afford **5a** as yellow powder (77.3 mg, yield 95 %). For **5a**, mp: 67-69 °C; ^1H NMR (400 MHz, CDCl_3): δ = 4.30-4.40 (m, 4H), 1.82-1.90 (m, 4H), 1.74-1.82 (m, 8H), 1.56-1.65 (m, 4H), 1.42-1.55 (m, 8H), 0.95-1.05 (m, 15H); ^{13}C NMR (100 MHz, CDCl_3): δ = 163.02, 163.08, 145.16, 134.19, 133.47, 131.37, 130.80, 130.45, 127.04, 73.69, 65.81, 65.51, 32.39, 30.64, 30.55, 19.25, 19.21, 13.88, 13.76, 13.75; IR (KBr Pellet): 1713 cm^{-1} (C=O); HRMS: calculated for $\text{C}_{42}\text{H}_{54}\text{S}_3\text{O}_{10} + \text{Na}^+$, 837.2771; found, 837.2786.



Compound **1b** (89 mg, 0.1 mmol) and TBHP (4 drops) were dissolved in CH_2Cl_2 (10 mL). The resulting mixture was stirred at 40 °C for 5 h. After cooled down to RT, the reaction was quenched by adding distilled water and extracted with CH_2Cl_2 (3×15 mL). The organic layers were combined and dried over anhydrous Na_2SO_4 , then concentrated under reduced pressure. The crude product was further purified by column chromatography on silica-gel (eluent, CH_2Cl_2 : petro ether, 2 : 1, v/v) to afford **5b** as yellow powder (76.6 mg, yield 80 %). For **5b**, mp: 72~74 °C; ^1H NMR (400 MHz, CDCl_3) δ = 4.26-4.35(m, 8H), 1.81-1.90(m, 4H), 1.72-1.80(m, 8H), 1.55~1.64(m, 4H), 1.55-1.64(m, 4H), 1.42-1.50(m, 8H), 0.96-1.05(m, 15H); ^{13}C NMR(100 MHz CDCl_3): δ =163.62, 163.08, 145.16, 134.19, 133.47, 131.37, 130.80, 130.45, 127.04, 73.69, 65.81, 65.51, 32.39, 30.64, 30.55, 19.25, 19.21, 13.88, 13.76, 13.75; IR (KBr Pellet): 1703 cm^{-1} (C=O); HRMS (m/z): $[\text{M}]^+$ calculated for $\text{C}_{42}\text{H}_{54}\text{Se}_3\text{O}_{10}+\text{H}^+$, 957.1293; found, 957.1285.



Compound **5b** (958 mg, 1 mmol) and NaOH (800 mg, 20 mmol) were dissolved in the mixed solvent of EtOH (20 mL) and H_2O (2 mL), then stirred under reflux for 2 h. The reaction was then acidified by adding HCl aqueous (3 N) at 0 °C, and extracted with CH_2Cl_2 (3×15 mL). The organic layers were combined and dried over anhydrous Na_2SO_4 , then concentrated under reduced pressure. The crude product was further purified by column chromatography on silica-gel (eluent, ethyl acetate) to afford **6b** as yellow powder (62.1 mg, yield 85 %). For **6b**, mp: 204-206 °C; ^1H NMR (400 MHz, CDCl_3) δ = 4.67 (s, 1H), 4.12 (t, J = 6.3 Hz, 4H), 1.46-1.35 (m, 4H), 0.83 (t, J = 7.4 Hz, 6H); ^{13}C NMR(100 MHz CDCl_3): δ =166.26, 165.97, 146.32, 141.63, 137.18, 136.41, 135.08, 132.28, 130.56, 73.08, 32.19, 19.04, 12.85; IR (KBr Pellet): 1695 cm^{-1} (C=O); HRMS (m/z): $[\text{M}]^+$ calculated for $\text{C}_{26}\text{H}_{22}\text{Se}_3\text{O}_{10}+\text{H}^+$, 732.8789; found, 732.8784.



Compound **6b** (365.5 mg, 0.5 mmol), *p*-toluidine (133.8 mg, 1.25 mmol), and DCC (1.03 g, 5 mmol) were dissolved in anhydrous THF (10 mL). The resulting mixture was stirred at 80 °C for 12 h under nitrogen. After cooled down to RT, the reaction was quenched by adding distilled water and extracted with CH₂Cl₂ (3 × 15 mL). The organic layers were combined and dried over anhydrous Na₂SO₄, then concentrated under reduced pressure. The crude product was further purified by column chromatography on silica-gel (eluent, CH₂Cl₂: petro ether, 1 : 2, v/v) to afford **3b** as yellow powder (50 mg, yield 30 %). For **3b**, mp: >300 °C; ¹H NMR (400 MHz, CDCl₃): δ (ppm) = 7.38 (d, *J* = 8.1 Hz, 4H), 7.20 (d, *J* = 8.2 Hz, 4H), 4.41 (t, *J* = 6.5 Hz, 4H), 2.46 (s, 6H), 1.92~1.83 (m, 4H), 1.58~1.66 (m, 4H), 1.03 (t, *J* = 7.4 Hz, 6H); ¹³C NMR (100 MHz, CDCl₃): δ (ppm) = 162.18, 161.92, 149.80, 149.01, 138.49, 136.45, 134.77, 133.95, 132.81, 130.42, 127.28, 73.56, 32.37, 29.69, 19.27, 13.85; IR (KBr Pellet): 1651 cm⁻¹ (C=O); HRMS: calculated for C₄₀H₃₂N₂O₆Se₃+H⁺, 874.8937; found, 874.9856.

3. Thermogravimetric Analyses (TGA)

The thermogravimetric analyses (TGA) of compounds **3a** and **3b** were conducted on 1090B type thermal analyzer (Dupont Engineering Polymers).

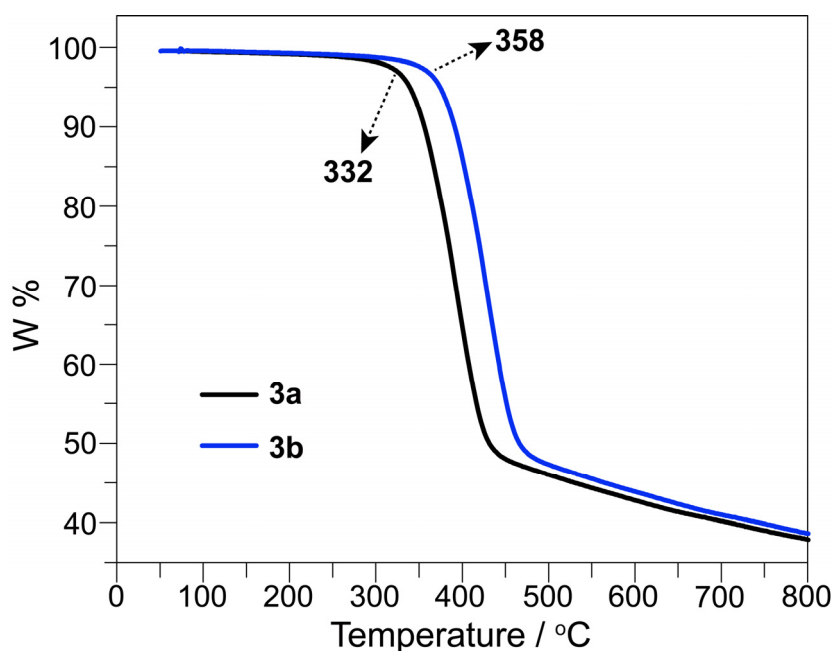


Fig. S1 Thermogravimetric analyses of the products **3a** and **3b**.

4. Theoretical calculation

All calculations were carried out with the *Gaussian 16* programs.^[S3] For DFT calculations, we used the hybrid gradient corrected exchange functional of Lee, Yang, and Parr.^[S4a, S4b] A standardized 6-311G basis set^[S4c] was used together with polarization (d) and (p) functions. In order to simplify the calculation, the *n*-butoxyl groups on **2a**, **2b**, **3a**, and **3b** were truncated to methoxyl groups, leading to **2a'**, **2b'**, **3a'**, and **3b'**, respectively. For the first singlet excited state calculation of **2a'**, **2b'**, **3a'** and **3b'**, geometry optimization and transition electric dipole moment calculation were carried out at B3LYP/6-311G(d,p)/IEFPCM(dichloromethane) (nstates=4, root=1) level of theory.

Table S1. The calculated energy level for the frontier orbitals for compounds **2a'**, **3a'**, **2b'**, and **3b'**.

Compounds	Energy levels / eV				
	HOMO-1	HOMO	LUMO	LUMO+1	$E_g^{[a]}$
2a'	-5.39	-4.86	-2.37	-1.39	2.49
3a'	-5.78	-5.26	-2.46	-2.42	2.80
2b'	-5.20	-4.76	-2.35	-1.35	2.41
3b'	-5.67	-5.16	-2.47	-2.34	2.69

[a] $E_g = E_{LUMO} - E_{HOMO}$

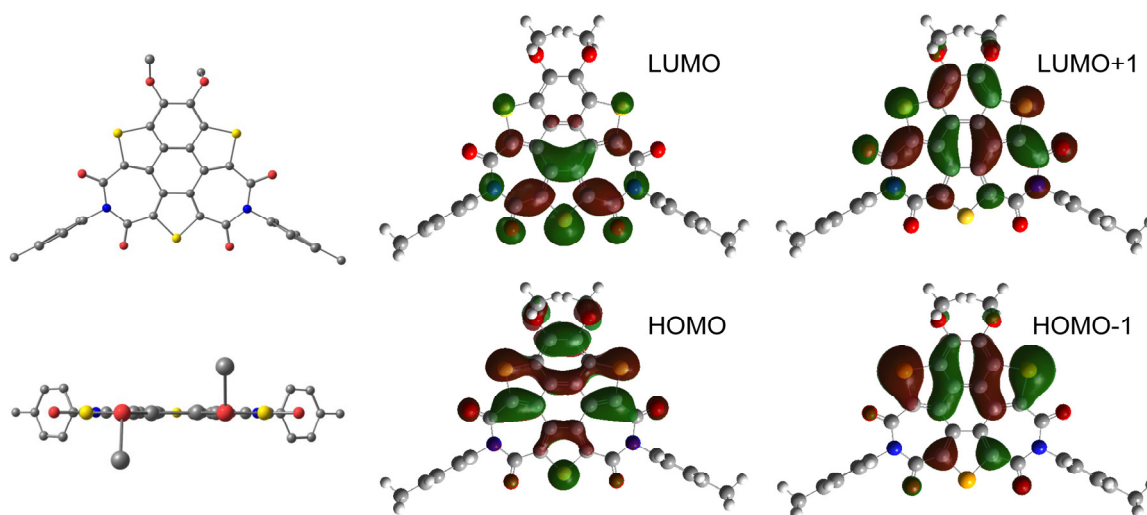


Fig. S2 Calculated molecular orbitals of compound **3a'**.

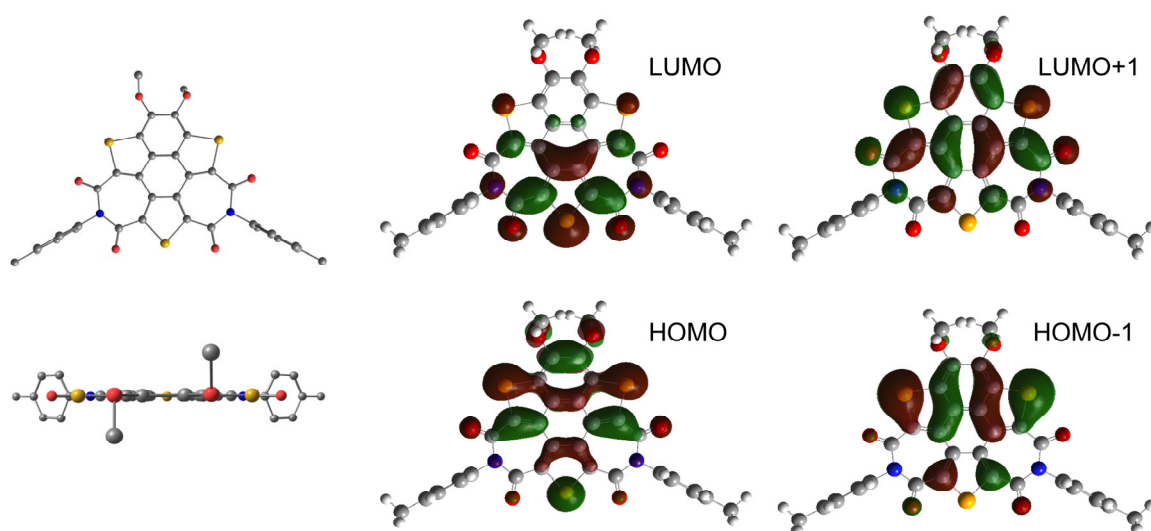
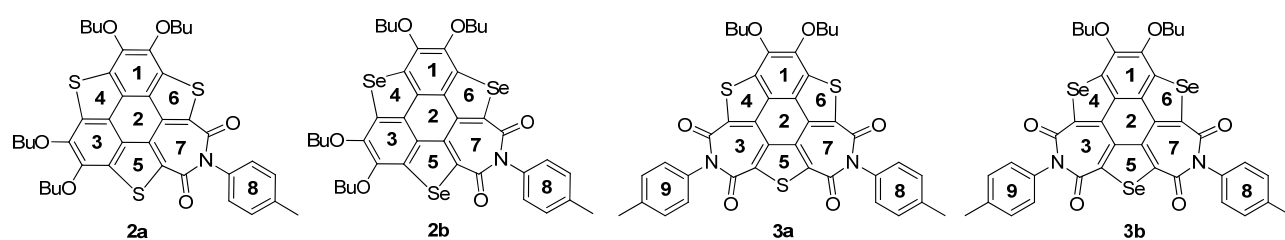


Fig. S3 Calculated molecular orbitals of compound **3b'**.

Table S2. NICS values of the representative compounds at the GIAO-B3LYP/6-311+G(d,p) level.



	1 ring	2 ring	3 ring	4 ring	5 ring	6 ring	7 ring	8 ring	9 ring
2a	-10.264	2.895	-10.263	-13.269	-14.186	-14.190	2.413	-8.111	-
2b	-9.613	3.481	-9.614	-11.533	-12.204	-12.201	2.453	-8.158	-
3a	-9.556	3.007	3.750	-15.772	-16.204	-15.770	3.750	-8.195	-8.195
3b	-9.382	3.660	3.470	-13.408	-13.903	-13.408	3.471	-8.247	-8.247

Table S3. Transition electric dipole moments (in a.u.) and oscillator strengths of **2a'** from ground state to the nth excited states.

n	X	Y	Z	$X^2+Y^2+Z^2$	oscillator strength
1	-0.0005	-0.0016	-2.1353	4.5593	0.2017
2	0.013	0.9559	-0.0006	0.9139	0.0618
3	-0.0006	0.0351	-0.0011	0.0012	0.0001
4	-0.0175	3.2366	-0.0021	10.4761	0.7896

Table S4. Transition electric dipole moments (in a.u.) and oscillator strengths of **2b'** from ground state to the nth excited states.

n	X	Y	Z	$X^2+Y^2+Z^2$	oscillator strength
1	0.0001	-0.0017	-2.2934	5.2598	0.2269
2	-0.0001	1.3479	-0.0006	1.8168	0.1159
3	0.0000	0.0050	0.0243	0.0006	0.0000
4	-0.0114	3.0027	-0.0015	9.0163	0.6658

Table S5. Transition electric dipole moments (in a.u.) and oscillator strengths of **3a'** from ground state to the nth excited states.

n	X	Y	Z	$X^2+Y^2+Z^2$	oscillator strength
1	0.8768	-0.0471	0.0021	0.7710	0.0310
2	-0.0067	-0.0030	2.9438	8.6662	0.4861
3	-0.0017	-0.0007	0.7019	0.4927	0.0339
4	0.0005	0.0000	-0.0680	0.0046	0.0003

Table S6. Transition electric dipole moments (in a.u.) and oscillator strengths of **3b'** from ground state to the nth excited states.

n	X	Y	Z	$X^2+Y^2+Z^2$	oscillator strength
1	-0.9856	0.0478	-0.0012	0.9737	0.0378
2	-0.0041	-0.0030	3.0832	9.5062	0.5192
3	0.0007	0.0003	-0.4906	0.2407	0.0150
4	-0.0002	-0.0001	0.0031	0.0000	0.0000

Meanwhile, the transition dipole moments between *i*th and *j*th excited states and corresponding energy differences in **3a'** and **3b'** were calculated according to the literature (T. Lu and F. Chen, *J. Comput. Chem.*, 2012, **33**, 580–592.).

Table S7. The transition dipole moments between *i*th and *j*th excited states (in a.u.) and corresponding energy difference (in eV) in **3a**'.

<i>i</i>	<i>j</i>	<i>X</i>	<i>Y</i>	<i>Z</i>	$X^2+Y^2+Z^2$	energy difference	oscillator strength
1	2	0.0044	0.0023	-2.0580	4.2352	0.7117	0.0739
1	3	0.0027	0.0010	-1.1848	1.4038	1.1263	0.0387
1	4	0.0003	0.0000	0.0203	0.0004	1.1786	0.0000
2	3	-0.0923	0.0004	0.0001	0.0085	0.4146	0.0001
2	4	0.0304	0.0241	-0.0027	0.0015	0.4669	0.0000
3	4	-0.1873	-0.0005	-0.0014	0.0351	0.0523	0.0000

Table S8. The transition dipole moments between *i*th and *j*th excited states (in a.u.) and corresponding energy difference (in eV) in **3b**'.

<i>i</i>	<i>j</i>	<i>X</i>	<i>Y</i>	<i>Z</i>	$X^2+Y^2+Z^2$	energy difference	oscillator strength
1	2	0.0028	0.0020	-2.1667	4.6945	0.7116	0.0818
1	3	-0.0023	-0.0017	1.6168	2.6139	0.9313	0.0596
1	4	-0.0012	0.0000	-0.0098	0.0001	1.2155	0.0000
2	3	0.0734	-0.0055	0.0003	0.0054	0.2197	0.0000
2	4	0.0022	-0.0010	0.0002	0.0000	0.5039	0.0000
3	4	0.0178	0.0116	-0.0020	0.0005	0.2842	0.0000

5. Photophysical properties

UV-Vis spectra were measured on UV-2006 UV-Specterophotometer. Fluorescence excitation and emission spectra were recorded with an RF-5301(pc)s Spectrofluorophotometer. Fluorescence lifetime and steady state were measured on FLS920 Spectrofluorophotometer.

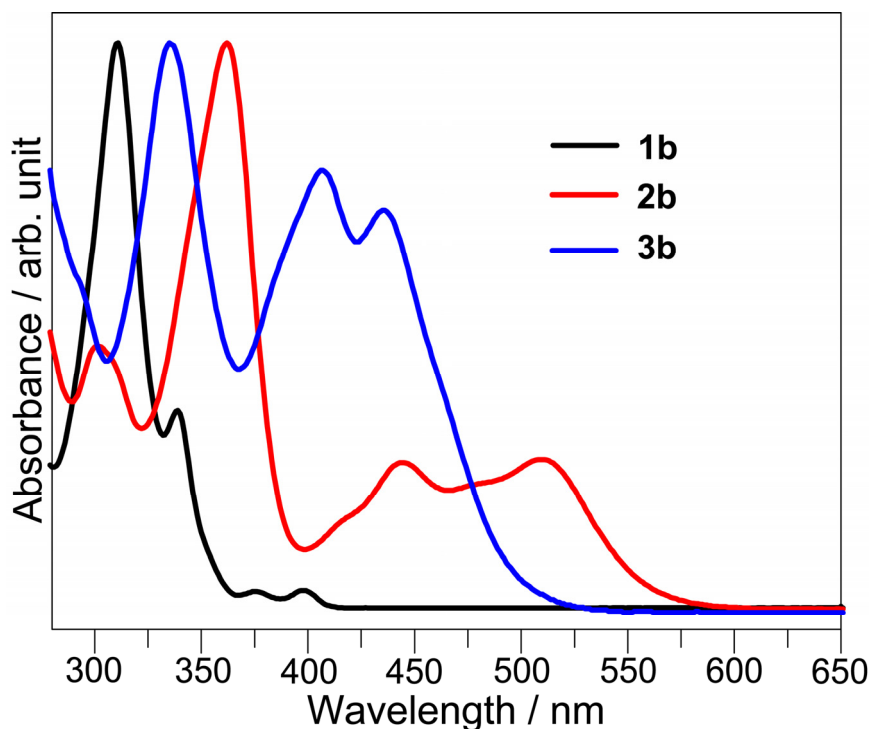
Table S9. UV/Vis absorption data for **1a–3b** in CH₂Cl₂ solution (*c* = 10⁻⁵ mol L⁻¹).

Compounds	λ_{\max}/nm	$\log \epsilon$	λ_{\max}/nm	$\log \epsilon$	λ_{\max}/nm	$\log \epsilon$
1a	312	4.94	344	4.40	—	—
2a	361	5.09	445	4.46	511	4.51
3a	319	4.63	390	4.49	419	4.48
1b	311	5.07	339	4.61	—	—
2b	363	4.97	446	4.37	512	4.38
3b	335	4.62	406	4.52	435	4.47

Table S10. The emission and excitation properties of **2a** and **3a** in CH₂Cl₂ solution^[a, b]

Compounds	λ_{ex} / nm	λ_{em} / nm	Stocks shift / cm ⁻¹	Φ_{F} / %
2a	340	637	13713	32.4
3a	420	540	5291	1.6

[a] Measurement conditions: $c = 10^{-5}$ mol L⁻¹, 20 °C; λ_{ex} : excitation wavelength; λ_{em} : maximum emission wavelength; Φ_{F} : fluorescence quantum yield

**Fig. S4** UV-Vis absorption of compound **1b-3b** in CH₂Cl₂ solution (10^{-5} mol L⁻¹) at 20 °C.

6. Electrochemical investigation

The electrochemical properties of **2a**, **2b**, **3a**, and **3b** were investigated by means of the cyclic voltammetry (CV) method. The measurement was conducted on a RST 5000 electrochemical workstation at a scan rate of 50 mV s⁻¹, with glassy carbon discs as working electrode, Pt wire as counter electrode, and SCE electrode as reference electrode. The concentration was 5×10^{-4} mol L⁻¹ in CH₂Cl₂ and the supporting electrolyte was (*n*-Bu)₄N•PF₆ (0.1 mol L⁻¹). The measurement was performed at 20 °C after bubbling the solution with N₂ gas for 15 min. The data were summarized in **Table S9** and the CV graphs were shown in **Fig. S5**.

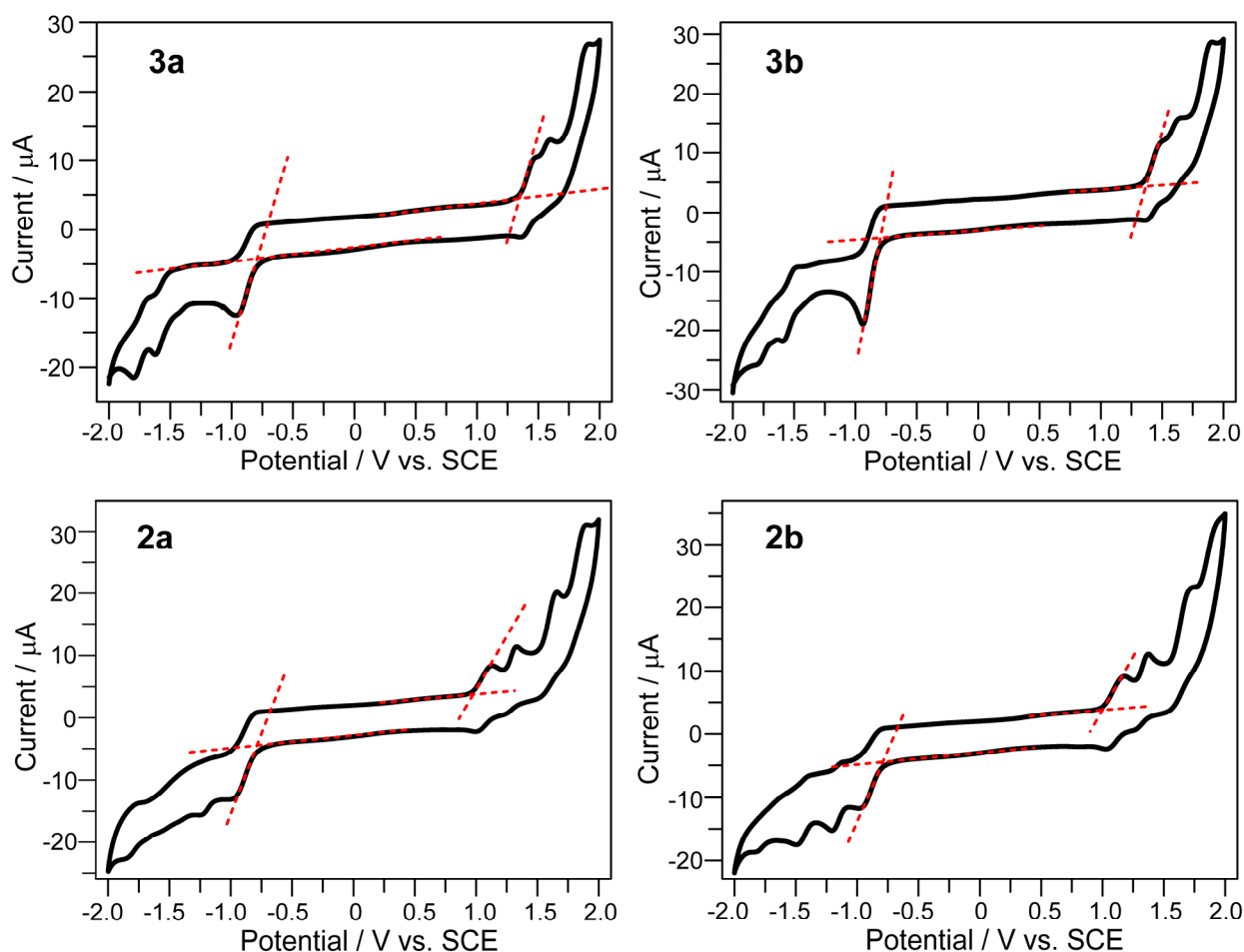


Fig. S5 cyclic voltammograms of **2a**, **2b**, **3a**, and **3b**. The red dashed lines are eye guide to the on-set of the first reduction and oxidation potentials.

Table S11. Electrochemical data, estimated HOMO and LUMO levels, and HOMO-LUMO gap.

	$E_{\text{on-set}}^{\text{red}}$	E_{LUMO}	$E_{\text{on-set}}^{\text{ox}}$	E_{HOMO}	E_{g} / [eV]	
	[V] ^a	[eV] ^b	[V] ^a	[eV] ^b	Electrochemical ^c	Optical ^d
2a	-0.77	-3.63	0.93	-5.33	1.70	2.16
2b	-0.78	-3.62	0.97	-5.37	1.75	2.13
3a	-0.79	-3.61	1.34	-5.74	2.13	2.45
3b	-0.79	-3.61	1.36	-5.76	2.15	2.41

^a $E_{\text{on-set}}^{\text{red}}$ and $E_{\text{on-set}}^{\text{ox}}$ respectively represent the on-set reduction and on-set oxidation potentials of the compounds;

^bThe HOMO and LUMO energy levels are estimated based on the electrochemical data, *i.e.*, $E_{\text{LUMO}} = -e (E_{\text{on-set}}^{\text{red}} + 4.40)$ (eV) and $E_{\text{HOMO}} = -e (E_{\text{on-set}}^{\text{ox}} + 4.40)$ (eV); ^c $E_{\text{g}} = E_{\text{LUMO}} - E_{\text{HOMO}}$; ^d E_{g} is calculated on the basis of the on-set of lowest absorption band.

7. Z-scan measurements

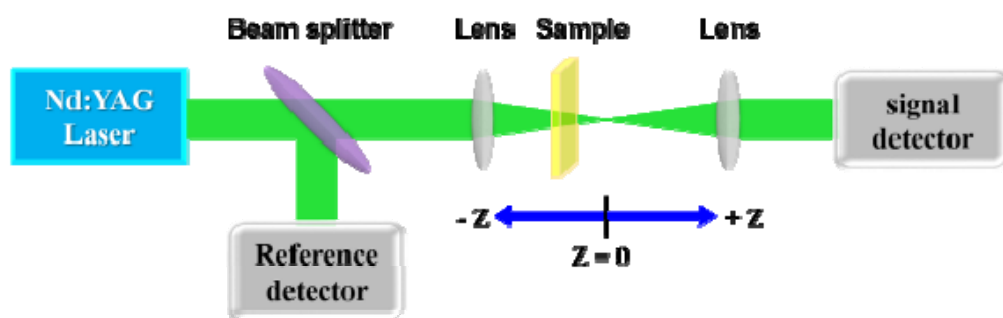


Fig. S6 The typical double-beams experimental arrangement of Z-scan measurement

The Z-scan method was introduced in 1989 by Sheik-Bahae *et al.*^[S3] using to determine the magnitude of the excited-state absorption cross-section (σ_{ex}), nonlinear absorption coefficient (β_{eff}) and the sign and magnitude of the nonlinear refractive index (n_2). In this work, the optical performances are collected using Z-scan technology with FWHM of 8 ns laser pulses with a repetition frequency of 10 Hz from a Nd:YAG laser (Spectra-Physics Quanta-Ray INDI Pulsed Nd:YAG Laser, optical parametric oscillator) under wavelength of 532. The spatial and temporal profiles of the laser pulses presented an approximately Gaussian distribution. As shown in Fig. S4, the laser beam has been divided into two beams: one laser beam is collected directly by reference detector to monitor energy fluctuations. Meanwhile, another beam is focused with lens on samples to detect the transmittance as the sample is scanned through the Z-direction to tune the intensities on it. Herein, the measurements were performed under open-aperture configuration. The Z-scan curves, the normalized transmittance as a function of sample position (Z), were measured with an open-aperture. We used normalized transmittance, which equals to the ratio of nonlinear and linear transmittance, as a standard to study the NLO properties of **2a**, **3a**, **2b**, **3b**, and C_{60} . For better comparison, the linear transmittance of the compounds were tuned into 70% under 532 nm by using a quartz cell with thickness of 5 mm before measurement. The samples were placed in quartz cell with thickness of 1 mm and fixed on a stepper motor which was controlled by a computer to move along the Z axis reference to the focal point. In this measurement, normalized transmittance of 1.0 indicates that the material exhibits no NLO behavior. When the sample exhibits saturable absorption (SA), normalized transmittance above 1.0 will be observed. The normalized transmittance below 1.0 indicates that the sample exhibits reverse saturable absorption (RSA). For optical limiters, the measured curves would exhibit valleys at the focus and the deeper the valley, the stronger the optical limiting performance of the material. Actually, as depicted in text, significant OL behaviors at broadband spectra with low limiting threshold and high NLO coefficients based RSA effect have been observed in the novel twisted π -conjugated D-A type molecule.

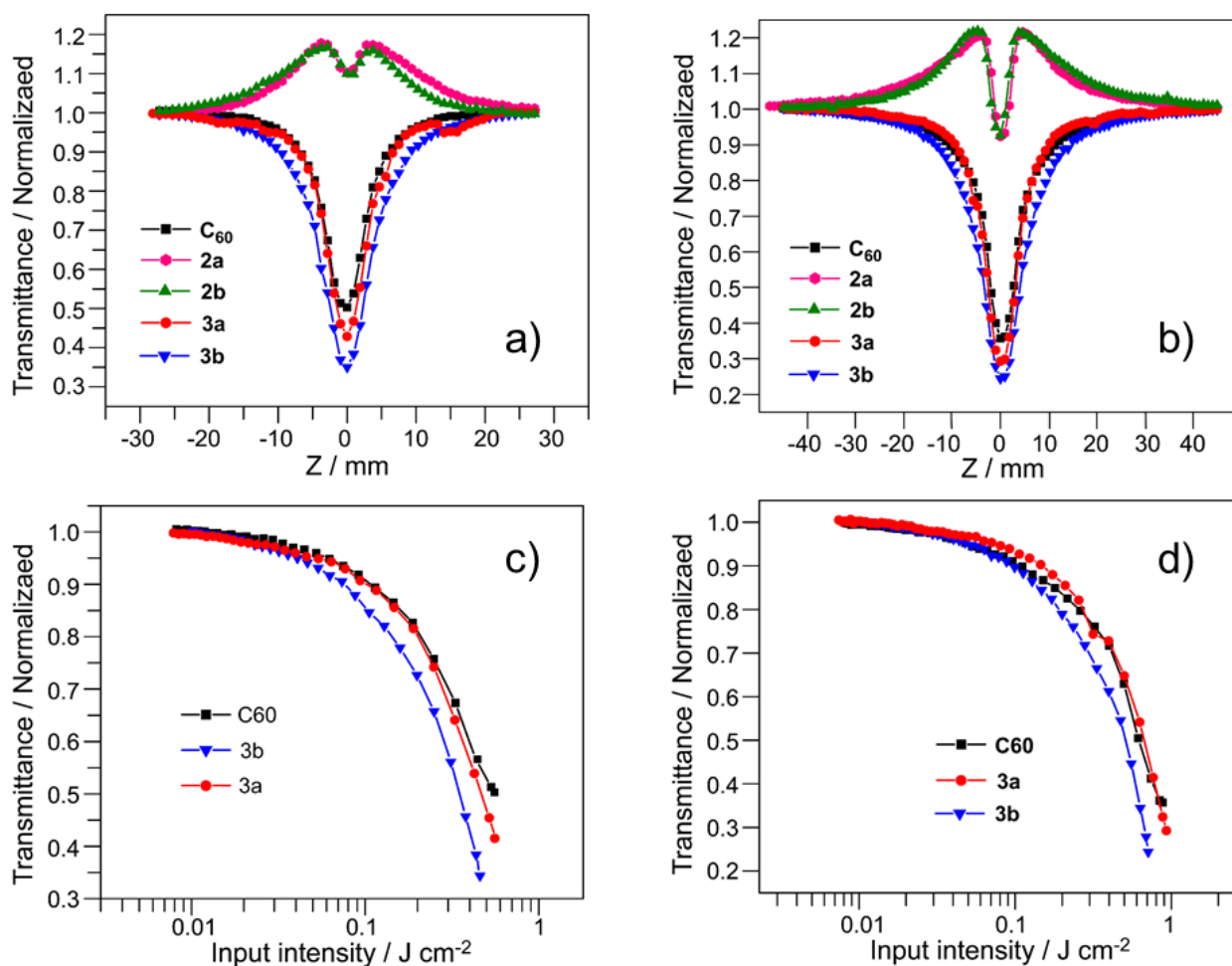


Fig. S7 Open aperture Z-scan for **2a**, **3a**, **2b**, **3b**, and C₆₀ under laser intensity of a) 10 μJ and b) 20 μJ; transmittance vs input fluence for **3a**, **3b**, and C₆₀ using c) 10 μJ and d) 20 μJ laser pulse. Measurement conditions: solvent, 1,1,2,2-tetrachloroethane (boiling point, 146 °C); linear transmittance, 0.70; laser pulse, λ = 532 nm, pulse width 8 ns

8. ^1H NMR, ^{13}C NMR and IR Spectra of products

